

The effects of substrate potentials on electron cyclotron resonance plasmas

S. M. Rosnagel, K. Schatz, S. J. Whitehair, R. C. Guarnieri, D. N. Ruzic et al.

Citation: *J. Vac. Sci. Technol. A* **9**, 702 (1991); doi: 10.1116/1.577347

View online: <http://dx.doi.org/10.1116/1.577347>

View Table of Contents: <http://avspublications.org/resource/1/JVTAD6/v9/i3>

Published by the AVS: Science & Technology of Materials, Interfaces, and Processing

Related Articles

Mass filtered plasma focused ion beam system

J. Vac. Sci. Technol. B **30**, 06F604 (2012)

On the scaling of rf and dc self-bias voltages with pressure in electronegative capacitively coupled plasmas

J. Vac. Sci. Technol. A **30**, 021303 (2012)

Spatially resolved study of primary electron transport in magnetic cusps

J. Vac. Sci. Technol. A **30**, 011301 (2012)

Low energy micron size beam from inductively coupled plasma ion source

J. Vac. Sci. Technol. B **29**, 051604 (2011)

200-mm-diameter neutral beam source based on inductively coupled plasma etcher and silicon etching

J. Vac. Sci. Technol. A **28**, 1169 (2010)

Additional information on *J. Vac. Sci. Technol. A*

Journal Homepage: <http://avspublications.org/jvsta>

Journal Information: http://avspublications.org/jvsta/about/about_the_journal


Top downloads: http://avspublications.org/jvsta/top_20_most_downloaded

Information for Authors: http://avspublications.org/jvsta/authors/information_for_contributors

ADVERTISEMENT


Instruments for advanced science

Gas Analysis




- dynamic measurement of reaction gas streams
- catalysis and thermal analysis
- molecular beam studies
- dissolved species probes
- fermentation, environmental and ecological studies

Surface Science




- UHV TPD
- SIMS
- end point detection in ion beam etch
- elemental imaging - surface mapping

Plasma Diagnostics



- plasma source characterization
- etch and deposition process reaction kinetic studies
- analysis of neutral and radical species

Vacuum Analysis




- partial pressure measurement and control of process gases
- reactive sputter process control
- vacuum diagnostics
- vacuum coating process monitoring

contact Hiden Analytical for further details

HIDEN ANALYTICAL

info@hideninc.com
www.HidenAnalytical.com

CLICK to view our product catalogue 

The effects of substrate potentials on electron cyclotron resonance plasmas

S. M. Rossnagel

IBM T. J. Watson Research Center, P.O. Box 218, Yorktown Heights, New York 10598

K. Schatz

University of Illinois, Champaign-Urbana, Illinois 60801

S. J. Whitehair and R. C. Guarnieri

IBM T. J. Watson Research Center, P.O. Box 218, Yorktown Heights, New York 10598

D. N. Ruzic

University of Illinois, Champaign-Urbana, Illinois 60801

J. J. Cuomo

IBM T. J. Watson Research Center, P.O. Box 218, Yorktown Heights, New York 10598

(Received 22 January 1991; accepted 28 January 1991)

In a conventional, axial electron cyclotron resonance (ECR) plasma source, the substrate is typically in the diverging magnetic field region immediately downstream from the ECR region. Due to the high electron mobility along magnetic field lines, the substrate potential may influence the properties of the plasma. A substrate electrode consisting of seven, individually biasable, concentric rings was positioned below the ECR source, such that the potential at the termination of the field lines could be controlled. The ECR source used was a commercial, 1.5-kW device operating at 2.45 GHz and utilized two large electromagnets to provide magnetic fields in the range of 200–1000 G. The plasmas were diagnosed by means of a microwave interferometer in the source region, an automated Langmuir probe, and an array of ground potential metal rings in both the source and sample regions of the chamber. The results suggest that ions in this source are poorly confined (by the magnetic field) while electrons are well confined. The electron density could be increased slightly by electron reflection from the substrate region, or could be depleted strongly by substrate potentials exceeding the floating potential. The net efficiency of these sources is low: only about 14% of the ion flux from the plasma is incident on the sample position. The rest of the ions are lost at the source walls.

I. INTRODUCTION

Electron cyclotron resonance (ECR) plasma sources developed for plasma processing technologies have received a great deal of interest in the past several years.^{1–5} As the field has matured, the number of different source geometries has decreased to a relatively modest group of commercially available sources. One such standard source is the axial field, cylindrical waveguide ECR source. This source is generally 10–15 cm in diameter with a length of 20–40 cm. Two or three large electromagnets are positioned along the major axis of the chamber to provide a magnetic field on the order of 1000 G near the microwave window, with the field decreasing to 100–300 G farther downstream at the sample position.

While the observed plasma densities in this type of source can exceed 10^{12} cm⁻³ and the ion current densities to a substrate plane outside the source region can be many mA/cm² or even several tens of mA/cm², the efficiency of these sources is low. Typically, a commercial ECR source might produce an ion saturation current of 2 A for an incident microwave power of 1500 W. This translates into an ion delivery cost of 750 eV/ion. This is well above the energy per delivered ion amount for a Kaufman-type broad-beam ion source, which might operate at 350 eV/ion. While there are major differences in terms of ion acceleration and confine-

ment, it remains that the energy cost for producing a delivered ion with an axial ECR source is high. This will result in high-power losses to the walls and the need for additional cooling.

The confinement of the ions in an ECR source is also dependent on the cyclotron motions of the ions and ion-neutral scattering. Depending on the energy of the ions and the position in the source, the orbits may vary significantly. In the ECR region (1000 G), ions with less than a few tenths of an eV have orbits of only a few millimeters. However, if the ion temperature rises to an eV or more, as has been reported in some cases,⁶ the orbit radius near the throat of the source can be several centimeters. This will result in a significant number of wall collisions for these ions. In addition, ion-neutral scattering at 1 mTorr results in a collision frequency on the order of the rotation frequency. Thus further reduces the confinement of the ions.

An additional feature which differentiates the axial ECR source from other ion sources is the strong magnetic field, typically as high as 1000 G near the microwave window and several hundred gauss at the sample position. It has been observed that probes inserted into the plasma perpendicular to the magnetic field tend to “sweep out” regions of the plasma upstream and downstream along the magnetic field lines. This can be observed visually as a shadowing or darkening along those field lines. It was also anticipated that the poten-

tial and conductivity of the sample would perturb the plasma due to the high electron mobility along field lines and that altering the potential distribution at the sample may be a means to control the spatial properties of the plasma.

II. EXPERIMENTAL STUDIES

A commercial 1.5-kW axial ECR system was used for this study.⁷ In this system, the chamber has a radius of 14 cm and a height of 40 cm and is water cooled. Two large electromagnets provide an axial field which peaks at about 1000 G at the quartz window, falls to about 300 G at the throat of the source, and falls to 100–200 G at the sample position 10 cm further downstream. The process gas, Ar, is inserted near the window at 50 sccm, and the pressure is maintained at 0.5–1 mTorr by an adjustable gate valve. The source chamber walls (metal) were grounded and no liner was used.

The sample electrode was constructed of several flat, concentric Cu rings, with a 2-mm gap between each set of rings. The largest diameter was 26 cm. The rings could be individually biased dc and the current measured. Additional electrodes in the form of thin metal rings were placed at the wall position in the source region as well as at the edge of the sample electrode. These electrodes were individually grounded through an ammeter. Figure 1 shows an approximate schematic of the source and sample region and the electrode positions. In addition, a modified version of a commercially available Langmuir probe was used at three locations in the chamber: in the source region just below the ECR zone, in the sample region about 5 cm above the sample, and vertically, on the axis of the machine, from the sample position up the throat of the source. In the first two of these locations, the cylindrical probe axis was perpendicular to the magnetic field lines. In the third case, the probe tip was bent at 90° such that the active region of the probe was perpendicular to the primary axis of the magnetic field. A microwave interferometer was also mounted across the upper ports in

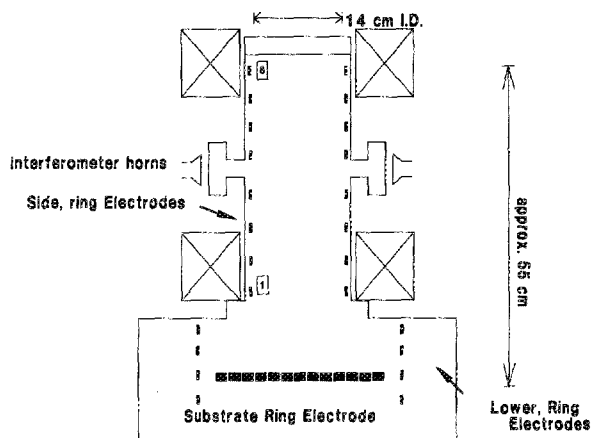


FIG. 1. Schematic of the experimental configuration showing the ECR source, the sample electrode, the two sets of side ring electrodes and the magnetic field coils. The interferometer was located at the two ports located between the magnetic field coils. The numbers by the rings in the source throat refer to the axis of Fig. 5.

the source region to provide a line-integrated density across the source. Due to the difficulty in analyzing Langmuir probe traces particularly in the presence of several hundred gauss magnetic fields, it is believed the absolute probe results are only accurate to about a factor of 2x. As an indication of this, the line-integrated interferometer signal tended to correlate moderately well with the observed densities measured with the Langmuir probe. It was, however, quite valuable to monitor the spatial dependence of the probe traces. This type of relative information was not available through the interferometer alone.

All experiments used an incident microwave power of 1000 W, tuned such that the reflected power was below 20 W. The magnetic field configuration was also kept constant and no third, downstream magnet was used. For some runs, quartz limiters with an inside diameter of 10.8 cm were used both at the throat of the source and in the source region. These limiters tended to intercept field lines which also intercepted nearby wall positions.

It should be noted that the magnetic field configuration on this source has a distinct bulge between the two magnet positions. The result of this bulge is that a sizeable fraction of the magnetic field lines intercept the grounded wall of the chamber in the source region. This feature of the configuration would not be present in a source which either had more magnets, or had a smaller length-to-diameter ratio. The microwave window became nonuniformly coated with metal films during extended operation of the source (< 30 min at 1 kW). The metal was most likely due to sputtering of the source walls near the window. Significant window coatings did not result in appreciable changes in reflected power, although it altered the electron density distribution in the source region. Care was taken to operate under clean window conditions by periodic cleaning of the window.

III. RESULTS

A. Substrate potentials and distributions

The floating potential of the substrate under the standard operating conditions (1000 kW at 2.45 GHz, 50 sccm Ar at 0.8 mT) averaged about -5 V. By biasing the seven-ring substrate assembly negative, it was possible to repel electrons and reach a simple ion saturation mode at about -15 to -20 V dc. Voltages more negative of this resulted in no additional ion current, but increased the probability of physical sputtering of sample electrode. The subject of low-energy sputtering has not been dealt with in this study. However, a related effort has begun to examine the sputter yields at ion energies well below the traditional threshold values.⁸ Significant fluxes of metal atoms can be generated in ECR plasmas even though the plasma potential or the ion energy remains well below 20 eV.

The effect on the overall plasma density up near the source region can be seen in Fig. 2. Here the electron density is measured by means of the interferometer. As seen in Fig. 2, voltages more negative of the floating potential result in modest increases in the electron density. By adjusting the sample electrode voltage to be more positive of the floating potential, electrons are drained from the plasma, and as a

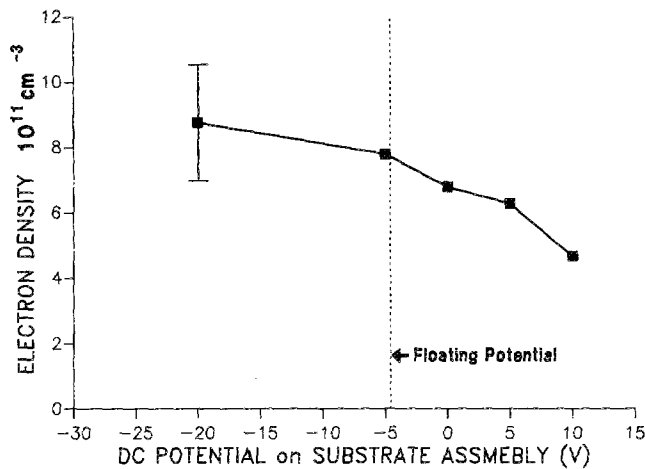


FIG. 2. Line-integrated (window-to-window) electron density in the ECR source region as a function of the potential on the entire substrate plate. The dotted line at about -5 V was the floating potential.

result, the source-region electron density drops significantly. This can also be seen in Fig. 3, in which the ion saturation current from the Langmuir probe is plotted as a function of chamber radius. At the floating potential, the density is centrally peaked. As the substrate voltage (all rings together) is powered more positive of the floating potential, the distribution becomes less peaked, although the magnitude of the ion saturation current drops significantly.

With the ability to power each of the rings individually, it is possible to selectively alter the profile of the plasma. This is shown in Fig. 4, where the center three rings (positions from 0 to 4.5 cm radius) have been set to 0 V (5 V more positive than the floating potential), and the outer four rings (positions from 4.5 to 10 cm radius) have been set to ion saturation (-20 V). The density profile of the plasma in the region above the sample reflects the draining of electrons from the central region. The plasma potential (lower plot, Fig. 4) is not altered by this density gradient within the accuracy of the measurement. This implies that ions have the same radial density profile as the electrons and that the net current to the wall will become more positive.

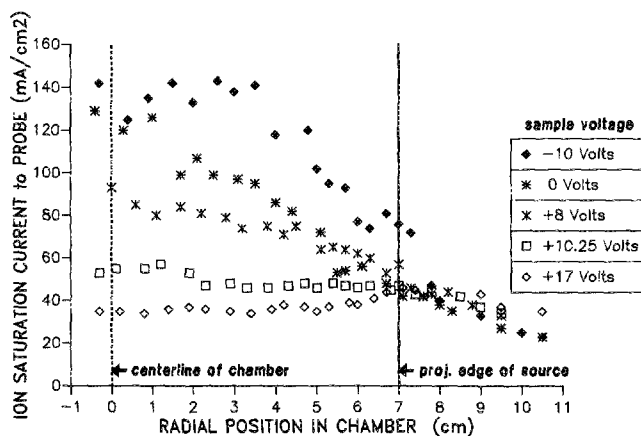


FIG. 3. Ion saturation current measured to the Langmuir probe as a function of radial position in the chamber. The probe location is 9 cm above the sample plane.

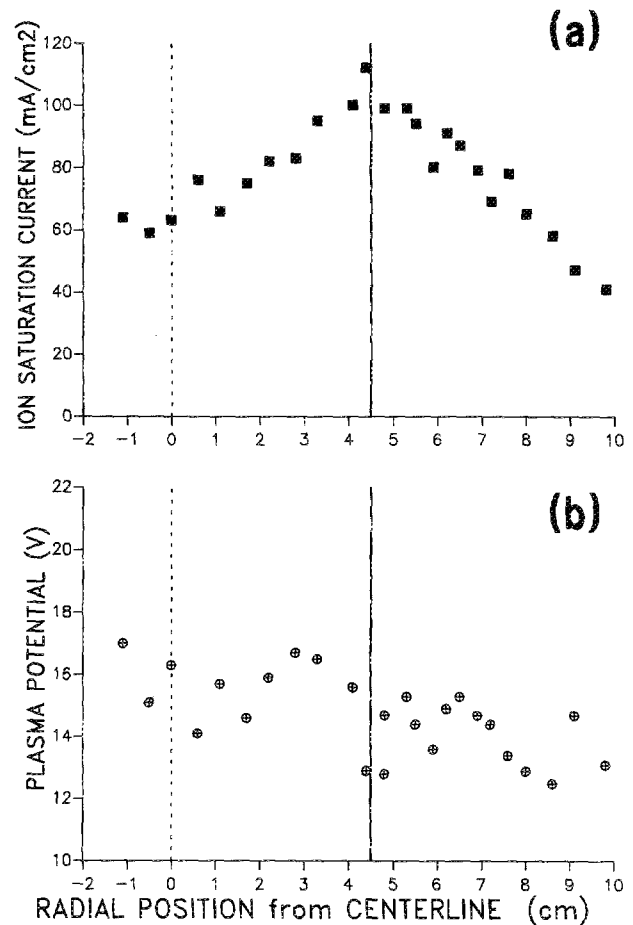


FIG. 4. (a) The ion saturation current to the Langmuir probe as a function of radial position in the chamber for the case of biasing the central three electrodes on the sample array (positions 0–4.5 cm radius) to 0 V (5 V above floating potential) and biasing the outer four ring electrodes on the sample (positions 4.5–10 cm radius) to -20 V (ion saturation). (b) The lower curve shows the plasma potential for these same positions.

B. Sampling rings in source region

There were eight metal rings set up near the wall in the source region. The rings were isolated from the grounded wall, but were themselves grounded through an ammeter such that the current to each could be measured. This type of measurement obviously includes both electron and ion currents: the net result is the sum of both. However, by systematically altering the potential on the sample plane and measuring the arriving currents, it is possible to estimate the relative ion and electron components to the rings in the source region.

Typical results are shown in Fig. 5 for the eight rings as a function of sample potential. (Ring 1 is near the throat of the source, and ring 8 is near the microwave window.) This initially surprising result is the very large electron currents to the wall for rings 6 and 7, which are near the ECR zone. However, these large electron currents can be explained by examining the magnetic field plots, which show a significant divergence of the magnetic field between the two electromagnets. Electrons streaming along field lines from the dense plasma near the window will intercept the wall at these

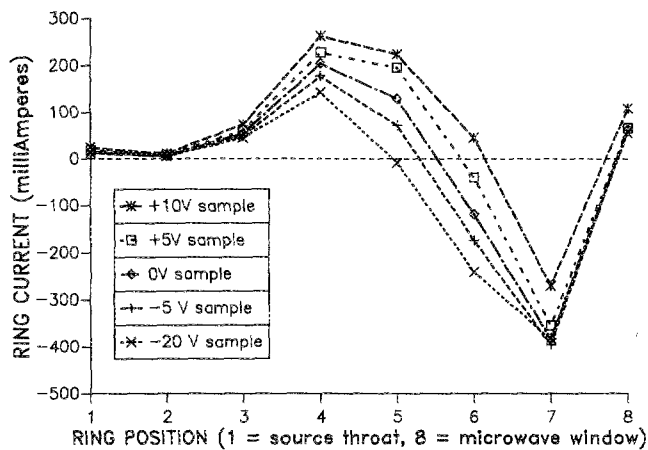


FIG. 5. Current to the ring electrodes near the wall in the source region as a function of position for several different voltages on the sample electrode (all rings). Ring 1 is located near the throat of the source, and ring 8 is near the microwave window.

positions. Indeed, significant wall damage, possibly enhanced by electron-current-induced heating, was observed in post-mortem analysis of similar sources.

By altering the sample potentials, the currents to the source wall could be predictably altered. By biasing the sample into ion saturation, the apparent electron current to the wall increased. By biasing the sample more positive, and drawing large electron currents to the sample, the net electron current to the wall reduces. Assuming that the ion flux to the wall in the source region is relatively isotropic, the net currents to the walls in the source region can be estimated by integrating the current measured at the probe along the length of the source (40 cm). The net electron current is about 10 A, and the net ion current is about 9 A. When the sample is in ion saturation, the total current to the sample is 1.2 A, and an additional 0.2 A is collected on the grounded rings adjacent to the sample. These values sum approximately to 0 A, as must be the case without any current sources to the discharge.

The net probability of an ion leaving the throat of the source is then about 14%, with the remainder of the ion and electron currents incident on the walls of the source region. In the case of total ion confinement, 50% of the ions would leave the source through the throat, with the remaining 50% incident on the microwave window. Therefore, the ion confinement is poor, resulting in a large fraction of the incident microwave power into the discharge being deposited on the walls in terms of the kinetic energies of both the ions (sheath potential about 14 V) and electrons ($kT_e \approx 5-6 eV$), as well as the recombination energy of the ions. This generally requires that the source walls be water cooled.

The magnetic field does increase the ion flow (14%) compared to the geometric opening of the source (8%), but the increase is small compared to the total ion current losses.

IV. DISCUSSION

The relatively low-emission probability for ions in this source (14%) suggests that ions are not well directed along

magnetic field lines, and are poorly confined. While the ion currents to the sample were larger than what would be expected simply from geometrical considerations (8%), they were significantly smaller than the level expected (50%) for total confinement, or "magnetization" of the ions. This result suggests that other processes, such as wall collisions and ion-neutral collisions, are important to the net directionality and magnitude of the ion flux in this source. It also suggests that the ambipolar acceleration along the vertical axis that should be expected due to the divergent magnetic field will be small. Preliminary measurements have shown a small axial potential gradient ($< 5 V$), compared to a sheath voltage of 13–17 V, in contrast to higher reported values.⁹

The imposition of a bias more negative than the floating potential does result in a very modest increase in electron density in the source region. The reason for the small increase is twofold: first, the reflected electrons must travel to a region of higher magnetic field, and, second, the radial transport and losses of electrons in these sources can be significant. This can be estimated by the observation of hollow discharges in the source region. The hollow profile is most probably due to a selective metal deposition in the center of the microwave window, and is observed with a spatially resolved Langmuir probe. However, at the sample location, the discharge is centrally peaked, indicative of radial transport for the electrons.

The imposition of a bias more positive than the floating potential results in significant electron losses from the plasma. The electron density profile can become flatter, but only at the expense of electron density. In addition, the plasma potential tends to ride up on top of a positive substrate bias, causing increased ion bombardment of the walls of the source.

Although density gradients and occasionally temperature gradients can be set up across the chamber due to selective biasing of individual rings on the sample electrode, the plasma potential remains approximately constant. Only a weak radial gradient in the potential (1–2 V decrease, center to edge sheath) was observed, with the strongest effect at the thin sheath at the wall (10–15 V). This can be viewed as a result of the relatively poor confinement of the ions, which tend to short out any radial variations, apart from the sheaths. Hence, even though the electron cross-field mobility is low enough to allow sizeable, local gradients in the density, the high mobility of the ions reduces any net change to the plasma potential.

The distinct bulge in the magnetic field in the region just below the ECR zone causes significant loss of the electron population. Virtually all of the electron current from the source (nearly 10 A) is deposited in this region onto the chamber walls. It is desirable to make the magnetic field more uniform through this region to reduce the electron losses. This may also serve to suppress the plasma potential, as now electrons would be required to diffuse across field lines to find ground.

The efficiency of the ECR source can be estimated by comparing the net ion current to the sample electrode to the total incident microwave power. Typically an ion saturation current of 1.2 A was measured for an applied power of 1000

W: an efficiency of 833 eV per ion.

Sources of this type, and also of the new Helicon type¹⁰ could be significantly improved by reducing the aspect ratio (length/diameter) of the source region. In fact, the ideal source would be a very low aspect ratio disk, in which 50% of the ions were able to leave the bottom of the source. Low aspect ratio sources are difficult to achieve with axial magnetic field geometry due to constraints on the magnetic field. An alternative geometry is to position the sample at the edge of the ECR zone, as is done with the Hitachi ECR system. In this case, the magnetic field is virtually uniform, and there is little concern with ambipolar potentials and uncertainties in the ion energy.

¹M. Matsuoka and K. Ono, *Appl. Phys. Lett.* **50**, 1864 (1987).

²M. Pinchot, A. Durandet, J. Pelletier, Y. Arnal, and L. Vallier, *Rev. Sci. Instrum.* **59**, 107 (1988).

³W. Holber, in *The Handbook of Ion Beam Processing Technology*, edited by J. J. Cuomo, S. M. Rossnagel, and H. R. Kaufman (Noyes, Park Ridge, NJ, 1989), Chap. 3.

⁴J. Asmussen, in *The Handbook of Plasma Processing Technology*, edited by S. M. Rossnagel, J. J. Cuomo, and W. D. Westwood (Noyes, Park Ridge NJ, 1990) Chap. 11.

⁵W. Holber and J. Forster, *J. Vac. Sci. Technol. A* **8**, 3720 (1990).

⁶J. S. McKillop, J. C. Forster, and W. M. Holber, *Appl. Phys. Lett.* **55**, 30 (1989).

⁷ASTeX Corporation, Woburn, MA.

⁸S. M. Rossnagel, D. N. Ruzic, and J. J. Cuomo (unpublished).

⁹D. J. Trevor, T. Nakano, N. Sadeghi, J. Derouard, R. A. Gottscho, P. D. Foo, and J. M. Cook, *J. Vac. Sci. Technol.* (to be published).

¹⁰R. W. Boswell, A. J. Perry, D. Vender, and H. B. Smith, *J. Vac. Sci. Technol.* (to be published).